

# THE NINE MORSE GENERIC TETRAHEDRA

D. SIERSMA AND M. VAN MANEN

**ABSTRACT.** From computational geometry comes the notion of a Gabriel graph of a point set in the plane. The Gabriel graph consists of those edges connecting two points of the point set such that the circle whose diameter is the edge does not contain any point of the point set in its interior. We define a generalization of the Gabriel graph to  $n$  dimensions: the Morse poset. Using Morse theory we prove that for a generic set of 4 points in  $\mathbb{R}^3$  there are nine different Morse posets, up to combinatorial equivalence. At the end we mention some open questions and report on the results of computer experiments concerning these. We also compare our shape classification to another criterion widely used in computer science.

## 1. INTRODUCTION

Take  $N$  points  $P_1, \dots, P_N$  in  $\mathbb{R}^n$  and consider the function  $d : \mathbb{R}^n \rightarrow \mathbb{R}$  defined by:

$$d(X) = \min_{j=1, \dots, N} d(X, P_j)$$

We want to study the evolution of the sets  $d_\epsilon = \{X \mid d(X) \leq \epsilon\}$ , as  $\epsilon$  increases. In particular we are interested in the Euler characteristic  $\chi$  of  $d_\epsilon$ . In case  $\epsilon$  is very small  $d_\epsilon$  consists of  $N$  small solid spheres. Thus  $\chi = N$ . If  $\epsilon$  is very big, then  $d_\epsilon$  is contractible and hence  $\chi = 1$ .

For a generic set of points,  $d$  is a topological Morse function. In that case, as  $\epsilon$  grows,  $d$  passes through a number of non-degenerate critical values. When  $d$  passes a critical value of index  $i$ , an  $i$ -cell gets attached.

The number of critical points of index  $i$  is  $a_i$ . From Morse theory we know that

$$\sum (-1)^i a_i = 1$$

As an example, take a triangle with an obtuse angle in the plane. This is a special case of the above problem with  $n = 2$  and  $N = 3$ . Assume further that the two legs that encompass the obtuse angle have different lengths. In that case  $a_0 = 3$ ,  $a_1 = 2$  and  $a_2 = 0$ . For an acute triangle where the edges have different lengths, we obtain  $a_0 = 3$ ,  $a_1 = 3$ , and  $a_2 = 1$ . In this sense, there are two different generic triangles.

Returning to the  $n$ -dimensional case, each critical point of index  $i$  corresponds to a subset of length  $i$  of  $\{P_1, \dots, P_N\}$ , but not every subset of length  $i$  corresponds to a critical point of index  $i$ . ( With the obtuse triangle the 2-face of the triangle, that is: the

---

*Date:* March 29, 2022.

*2000 Mathematics Subject Classification.* Primary 51M20; Secondary 68U05.

*Key words and phrases.* Morse theory, polyhedra, Voronoi diagram, tetrahedral shape.

triangle itself, does not correspond to a local maximum of the function  $d$ . ) The subsets of length  $i$  that do correspond to critical points of  $d$  will be called *active*. An active subset defines a geometric  $(i - 1)$ -simplex which we also will call *active*. Thus to the  $N$ -point set  $P_1, \dots, P_N$  we can associate a set of subsets that are the active faces. This set of subsets is partially ordered by inclusion, and thus it is a poset. We will call it the *Morse poset*.

*Question:* in  $\mathbb{R}^n$ , for generic sets of  $N$  points, how many different Morse posets are there, up to combinatorial equivalence?

When  $N = n + 1$  we thus ask how many “different” generic simplices there are. This is a natural first problem to consider.

In the plane the answer is two, see [Sie99] section 2. For obtuse triangles, the Morse poset is

$$\{\{P_1\}, \{P_2\}, \{P_3\}, \{P_1, P_3\}, \{P_2, P_3\}\}$$

and for acute triangles, we get the Morse poset

$$\{\{P_1\}, \{P_2\}, \{P_3\}, \{P_1, P_2\}, \{P_1, P_3\}, \{P_2, P_3\}, \{P_1, P_2, P_3\}\}.$$

The main theorem of this article says that in  $\mathbb{R}^3$ , there are nine different generic tetrahedra (3-simplices).

In the first section, we recall the relevant Morse theory. Then we establish some notation and state what Voronoi diagrams and Gabriel graphs are. Next, we state and prove the main theorem. In the last section we discuss transitions in relation to the configuration space of four points in  $\mathbb{R}^3$ . We also report on numerical experiments concerning volume data of the different compartments of the configuration space where the Morse poset is of a certain type. Finally we compare our classification to the classification by shape types in [Ede01].

## 2. GENERICITY CONDITIONS

We focus here on 4 points in  $\mathbb{R}^3$ , but most of the notations and definitions have straightforward extensions to the  $(n, N)$  general case.

We write  $P_{ij}$  for the middle of the interval  $P_i P_j$ ,  $P_{ijk}$  for the center of the circumscribed circle of the triangle  $P_i P_j P_k$ , and  $P_{1234}$  for the center of the circumscribed sphere of the tetrahedron. For the tetrahedron itself, that is to say the convex hull of  $\{P_1, P_2, P_3, P_4\}$ , we will use the notation  $\mathbb{T}$ .

We impose the following

**Genericity condition 2.1.** We require the set of points  $P_1, P_2, P_3, P_4$  to be in general position, so that the convex hull of  $P_1, P_2, P_3, P_4$  is 3-dimensional. Moreover the points  $P_{ijk}$  do not to lie on one of the edges of the triangle  $P_i P_j P_k$  and also  $P_{1234}$  does not lie in one of the planes of the triangles  $P_i P_j P_k$ .

The condition 2.1 means that the function  $d$  is not too badly behaved. To express more carefully what that means we recall the definition of a topological Morse function, see [Mor59]. Let  $P \in \mathbb{R}^n$ . And let  $f$  be a continuous real-valued function on  $\mathbb{R}^n$ .

**Definition 2.2.**  $f$  is topologically regular at  $P$  if there is some neighborhood  $U$  of  $P$  and a homeomorphism  $\phi: U \rightarrow \mathbb{R}^n$  such that one of the components of  $\phi$  is  $f$ . The function  $f$  has a critical point at  $P \in \mathbb{R}^n$  if  $f$  is not topologically regular at  $P$ . In that case,  $P$  is called a non-degenerate critical point of index  $i$  if there is a neighborhood  $U$  of  $P$  and a homeomorphism  $\phi: U \rightarrow \mathbb{R}^n$  such that

$$f \circ \phi = f(P) - \sum_{j=1}^i x_j^2 + \sum_{j=i+1}^n x_j^2$$

A topological Morse function is a continuous function that has only non-degenerate critical points.

For topological Morse functions the two crucial statements that hold in the differentiable case - the regular interval theorem and the attachment of cells, see chapter 5 in [Mil63] - are true as well, as Morse proves in [Mor73]. So if we show that  $d$  is topologically regular, we can apply those theorems, just as was done in [Sie99].

We will need the following notations:

Let

$$\text{Terr}(P_i) = \{X \in \mathbb{R}^3 \mid d(X, P_i) \leq d(X, P_k) \text{ for all } k\},$$

and  $V_i = \text{Terr}(P_i)$ ,  $V_{ij} = V_i \cap V_j$  ( $i$  different from  $j$ ),  $V_{ijk} = V_i \cap V_j \cap V_k$  (all three  $i, j, k$  different),  $V_{1234} = V_1 \cap V_2 \cap V_3 \cap V_4$ .

**Proposition 2.3.** *The function  $d$  is a topological Morse function if the condition 2.1 is fulfilled. In that case,  $d$  is topologically regular in all points of  $\mathbb{R}^3$ , except in  $P_1, P_2, P_3, P_4$ , where  $d$  has a minimum and (perhaps) in the points  $P_{ij}$ ,  $P_{ijk}$  and  $P_{1234}$ . Moreover  $d$  has*

- a minimum exactly in the points  $P_1, P_2, P_3, P_4$
- a 1-saddle (saddle point of index 1) in  $P_{ij}$  iff.  $P_{ij} = V_{ij} \cap P_i P_j$
- a 2-saddle (saddle point of index 2) in  $P_{ijk}$  iff.  $P_{ijk} = V_{ijk} \cap P_i P_j P_k$
- a maximum in  $P_{1234}$  iff.  $P_{1234} = V_{1234} \cap \mathbb{T}$ , equivalently  $P_{1234} \in \mathbb{T}$ .

*Proof.* If  $x = P_i$  then because the points lie in general position all  $P_j$  with  $i \neq j$  lie at some positive distance from  $x$ , so  $d$  has a minimum there. If  $x \in \text{Terr}(P_i)$  but  $x \neq P_i$  then  $x$  is obviously topologically regular.

The function  $d$  restricted to the interior  $V_{ij}$  has a minimum if  $P_{ij}$  lies in that interior. This can only happen when  $P_{ij} \neq P_{ijk}$ , which is assured by 2.1.

In the directions, orthogonal to  $V_{ij}$ ,  $d$  decreases so we see that  $d$  has a critical point of index 1 at  $P_{ij}$ .

The function  $d$  restricted to the interior of  $V_{ijk}$  has a minimum at  $P_{ijk}$  if  $P_{ijk}$  lies in that interior. This can only be the case when  $P_{ijk} \neq P_{1234}$ . In the directions orthogonal to  $V_{ijk}$   $d$  decreases, so  $d$  has a critical point of index 2 at  $P_{ijk}$ .

Finally if  $P_{1234} = V_{1234}$ ,  $d$  obviously has a maximum there. □

**REMARK 2.4.** Closer inspection might yield that 2.1 is actually not necessary. See [Sie99] for the 2-dimensional case.

Throughout this article we will always assume that point sets satisfy the genericity condition 2.1.

If  $d$  has a critical point as described by the conditions of the proposition 2.3 then we say that the corresponding center is *active*. As explained in the introduction, an active center determines a subset of the points  $P_1, P_2, P_3, P_4$ , which we call *active subset*. The *Morse poset* is the set of active subsets. Two sets of points in  $\mathbb{R}^3$  are called *combinatorially equivalent* if there exists a bijection, that sends the active subsets onto each other. We want to give a classification with respect to this equivalence relation.

### 3. MORSE THEORETIC POSSIBILITIES

From proposition 2.3 we know the maximal number the critical points of each type. Moreover the Euler characteristic should be  $+1$ . This gives a priori the following 9 possibilities:

$m$	$s1$	$s2$	$M$
4	6	4	1
4	5	3	1
4	4	2	1
4	3	1	1
4	2	0	1
4	6	3	0
4	5	2	0
4	4	1	0
4	3	0	0

But not all possibilities will occur. Since we start with 4 points and the result should be a connected space, we need at least 3 saddle points of index 1. This rules out the possibility  $(4, 2, 0, 1)$ .

We remind the reader that the definitions that follow assume the genericity condition 2.1. For the more general definitions see [BKOS97] or [Ede01].

The *Voronoi tessellation* of a point set  $\{P_1, \dots, P_N\}$  in  $\mathbb{R}^n$  consists of the union of the sets  $\text{Terr}(P_i)$ , together with their natural combinatorial structure. Its  $(n - 1)$ -skeleton consists of the intersections  $\text{Terr}(P_i) \cap \text{Terr}(P_j)$  and is usually called the *Voronoi diagram*. The *Delaunay "triangulation"* of that point set is the simplicial complex dual to the Voronoi tessellation. Its 1-skeleton consists of the line segments

$$\{P_i P_j \mid \dim(\text{Terr}(P_i) \cap \text{Terr}(P_j)) = n - 1\}$$

The *Gabriel graph* ( see [BKOS97], where it is defined in  $\mathbb{R}^2$  ) of a point set in  $\mathbb{R}^n$  is formed by using the points as vertices and placing an edge between two vertices exactly when the sphere, whose diameter is given by that edge, does not include any point from the set. The Gabriel graph is a subset of the Delaunay triangulation. Clearly the Gabriel graph is always connected.

Our Morse poset is related to these much-used notions from computational geometry as follows. If in our case the edge between  $P_i$  and  $P_j$  is part of the Gabriel graph then, the point  $P_{ij}$  is a saddle point of  $d$ . The Morse poset is a generalization of the Gabriel

graph. The Gabriel graph consists of the active subsets of length 2. Two Morse posets can only be combinatorially equivalent if the underlying Gabriel graphs are the same.

#### 4. ACTIVITY CONDITIONS

We list in figure 1 the (a priori) possible Gabriel graphs for the above cases, they are the connected graphs with 6 vertices. Just as the case  $(4, 2, 0, 1)$  can not occur, we will

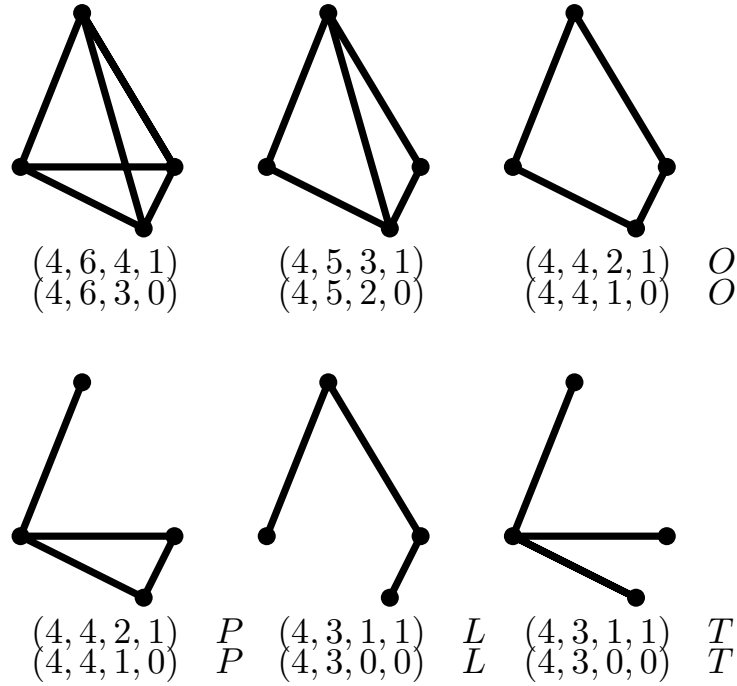


FIGURE 1. List of graphs

prove in this section by deriving a contradiction that the case  $(4, 4, 2, 1) P$ ,  $(4, 3, 1, 1) T$  and  $(4, 3, 1, 1) L$  do not occur. We will prove our main theorem:

**Theorem 4.1.** *Up to combinatorial equivalence of their Morse posets there are nine generic tetrahedra. They are uniquely described by the nine Gabriel graphs  $(4, 6, 4, 1)$ ,  $(4, 6, 3, 0)$ ,  $(4, 5, 3, 1)$ ,  $(4, 5, 2, 0)$ ,  $(4, 4, 2, 1) O$ ,  $(4, 4, 1, 0) O$ ,  $(4, 4, 1, 0) P$ ,  $(4, 3, 0, 0) L$  and  $(4, 3, 0, 0) T$ , drawn in figure 1.*

*Proof.* In the three cases that are to be excluded  $P_1P_2P_3P_4$  and  $P_1P_2P_3$  are active. Let us see what these two conditions mean.

**4.1. Saddle points of index 1.** We consider the plane  $E$  through  $P_1P_2P_3$  (and put is as ‘ground plane’ in the picture). The half space containing  $P_4$  is called ‘above’, the other is called ‘below’.

We are going to consider the condition that the point  $Y = P_{i4}$  is *active*. We first make no assumptions about the triangle  $P_1P_2P_3$ , except that it does not have a right angle. We

consider the point  $X = P_4$  as a variable and denote its projection on the  $E$ -plane by  $X'$ . Let  $Y = P_{14}$  and its projection  $Y'$ . From the condition that  $Y = P_{14}$  is active we get:

$$d(P_1, Y) = d(P_4, Y) \leq \min \{d(P_2, Y), d(P_3, Y)\}$$

For the projection, this means that in terms of Voronoi diagrams in  $E$ ,

$$Y' \in \text{Terr}(P_1)$$

In terms of the projection  $X'$ , this means:

$$X' \in 2 \text{Terr}(P_1),$$

where with  $2 \text{Terr}(P_1)$  we mean scalar multiplication of  $\text{Terr}(P_1)$  by a factor 2 from the point  $P_1$ .

We can do the same for the activity of  $P_{24}$  and  $P_{34}$ . We get three subsets  $2 \text{Terr}(P_1)$ ,  $2 \text{Terr}(P_2)$ ,  $2 \text{Terr}(P_3)$ , which cover the plane  $E$ . They divide the plane into regions, where one, two or three of the points  $P_{14}$ ,  $P_{24}$  or  $P_{34}$  are active.

Inside the plane  $E$ , the border of  $\text{Terr}(P_i)$  consists of two half-lines that meet in  $P_{123}$ . The scalar multiplication by two maps  $P_{123}$  to  $P_i^*$ , the antipodal point of  $P_i$  on the circle through  $P_1$ ,  $P_2$  and  $P_3$ .

Next, look at the case of an acute triangle drawn in figure 2.

The regions where only one  $P_{i4}$  is active are both outside the disc  $D$ , which is bounded by the circumscribed circle of triangle  $P_1P_2P_3$ .

The picture for the obtuse case is in figure 3.

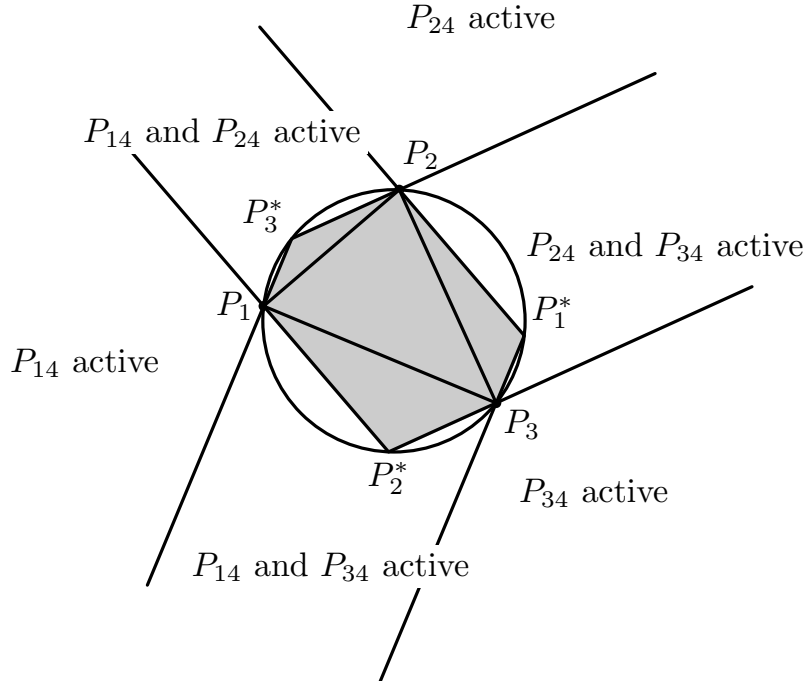
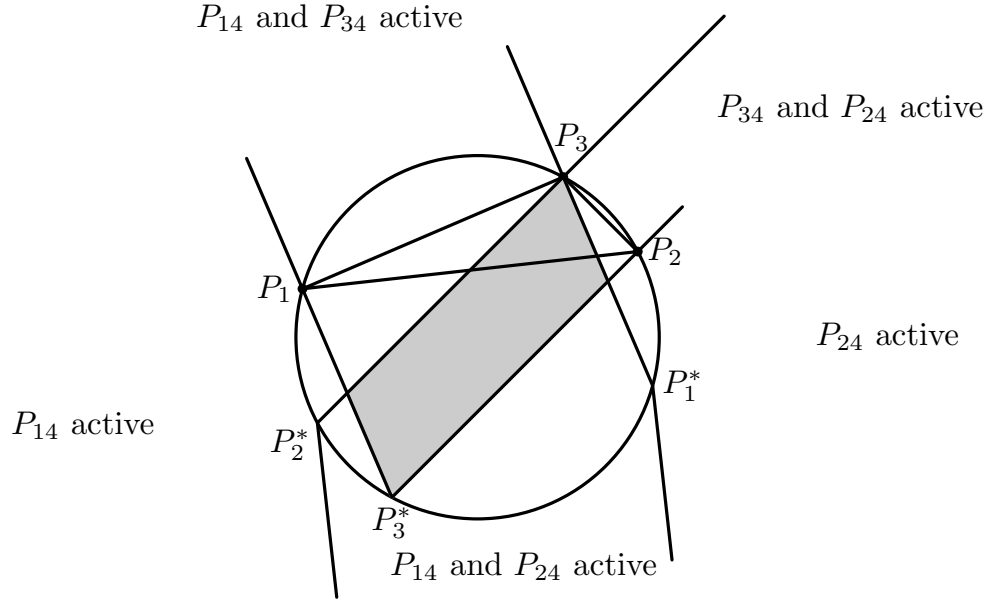


FIGURE 2. The plane  $E$  when the triangle is acute

FIGURE 3. The plane  $E$  when the triangle is obtuse

Let  $P_3$  the obtuse angle. We see that the region where only  $P_{34}$  is active is outside  $D$ , but that the regions where  $P_{14}$  or  $P_{24}$  is the only active saddle point can have some intersections with  $D$ .

**4.2. The center  $M$  of the circumscribed sphere.** We assume again that  $P_1P_2P_3$  lies in the plane  $E$ . We know that  $M = P_{1234}$  belongs to the axis of the triangle  $P_1P_2P_3$ , so its projection is  $M' = P_{123}$ . Fix  $M$  for the moment, and consider  $X = P_4$  as a variable. Possible positions of  $X = P_4$  are on the sphere with center  $M$  and radius  $r = d(P_1, M) = d(P_2, M) = d(P_3, M)$ . Denote by  $P_1^*P_2^*P_3^*$ , the mirror image of  $P_1P_2P_3$  after central reflection through  $P_{123}$ .

In the cases we wish to exclude,  $M$  is active, i.e.  $M$  is a point, where the distance function has its maximum, i.e.  $M$  lies inside the tetrahedron. The point  $X$  must lie in the cone with top  $M$  and base the triangle  $P_1P_2P_3$ , but also on the sphere  $(M, r)$ . Consider the the plane  $E''$ , which is the image of  $E$  by central reflection through  $M$ .  $E''$  is parallel to  $E$ . The cone intersects the plane in a triangle, which projects (orthogonally) exactly onto  $P_1^*P_2^*P_3^*$ .  $X$  belongs to a part of the cap of the sphere, which lies “above”  $E$  (seen from  $M$ ). It follow that  $X$  projects to a point  $X'$  which lies inside the disc  $D$ . (NB. the projection area contains at least the triangle  $P_1^*P_2^*P_3^*$ .) This is true for any position of  $M$ .

**4.3. Certain cases don't exist.** For the acute case this is all we need. In the obtuse case though we can be more precise. Let  $P_3$  be the obtuse angle. It is necessary for the activity of  $M$  that  $X'$  belongs to the circle sector  $P_2^*M'P_1^*$  (the one which does not contain  $P_3$ ). We combine the activity conditions for  $M$  and one single  $P_{i4}$ .

Start with an acute triangle in the ground plane. It follows that the combination  $M$  active and a single  $P_{i4}$  active can not occur together.

This rules out the graphs:  $(4, 3, 1, 1) T$ ,  $(4, 3, 1, 1) L$  and  $(4, 4, 2, 1) P$ .

**4.4. Positions of index 2 saddles.** We are left with nine possibilities of Gabriel graphs. The Gabriel graphs do not give a complete picture of the combinatorics of the Morse points. The Gabriel graph, together with the information about activity of  $M$ , tells us only the number of saddles of index 2, but not the position. We discuss this now in detail and show that there are in all cases unique positions for the saddles.

$(4, 6, 4, 1)$  : unique places (no choices).

$(4, 5, 3, 1)$  : There are two triangles, where all three midpoints are active. Both triangles must be acute. Take one of them in the ‘ground plane’ and assume it to be  $P_1P_2P_3$ . Since  $P_{1234}$  is active,  $P_{1234}$  lies on the same side as  $P_4$ . It follows that  $V_{123}$  must intersect the ground plane in the point  $P_{123}$ , so that point is active. The same reasoning applies to the second triangle; this fixes the place of two 2-saddles. The two positions left for the third saddle are combinatorially equivalent.

$(4, 4, 1, 0) O$  : all places equivalent.

$(4, 4, 2, 1)$  : Suppose  $P_{12}$  is not active. Now  $P_3$  or  $P_4$  must be contained in  $B = B(P_{12}, r_{12})$ , where  $r_{12} = d(P_1, P_{12})$ . If  $P_{123}$  is active, then triangle  $P_1P_2P_3$  must be acute, this means that  $P_3$  is outside the ball  $B$ . If  $P_{124}$  is active, then triangle  $P_1P_2P_4$  must be acute; this means that  $P_4$  is outside the ball  $B$ . It follows that the situation where two active 2-saddles are “separated” by an non-active edge cannot occur. This fixes the places of the 2-saddles up to permutation.

$(4, 6, 3, 0)$  : Since all midpoints of ribs are active, we have that all triangles are acute. Since  $P_{1234}$  is not active it lies outside  $\mathbb{T}$ . There is exactly 1 triangle such that  $P_{1234}$  and  $P_4$  lie on different sides of the plane of that triangle. The corresponding  $P_{ijk}$  on that axis cannot be active. This fixes the places of the other 2-saddles.

$(4, 5, 2, 0)$  : Choose a triangle, say  $P_1P_2P_3$ , where all three edges are active. If  $P_{123}$  is not active, then it follows that  $P_{1234}$  lies below the ground plane  $E$ . We look again at the projection  $P'_4$ . First  $P'_4$  must lie inside  $D$ . But since two of the  $P_{i4}$  (say  $P_{14}$  and  $P_{24}$ ) must be active we know that  $P'_4$  also must lie in the activity region, described above. The intersection is a subset of  $D$ , which is contained in the region  $D^*$  bounded by the arc  $P_1P_3P_2$  and the interval  $P_2P_1$ . There are still other conditions to meet:

- $P_4$  must lie outside the ball  $B(P_{12}, r_{12})$ , since  $P_{12}$  is active.
- $P_4$  must lie inside the ball  $B(P_{123}, r_{123})$ , where  $r_{123} = d(P_1, P_{123})$ .

This is not simultaneously possible if  $P'_4$  lies in  $D^*$ . It follows that there is only one possibility: the 2-saddles are the centers of two triangles with all edges active.

$(4, 4, 1, 0) P$  : Let  $P_1P_2P_3$  be the triangle with all three midpoints of the edges active. This triangle is acute, take its plane as ground plane. If  $P_{1234}$  is above the ground plane, then  $P_{123}$  is active. Assume now  $P_{1234}$  is below the ground plane. It follows that  $P'_4$  lies inside the disc  $D$ . But the fact that only  $P_{14}$  is active means that  $P'_4$  is outside. This is a contradiction, so only  $P_{123}$  can be active.

$(4, 3, 0, 0) T$  : all places equivalent.



$(4, 3, 0, 0) L$  : all places equivalent.

That all these cases do occur follows from the computer experiments described below. The proof of theorem 4.1 is complete.  $\square$

## 5. NOTES AND REMARKS

**5.1. Higher dimensional results.** We have not been able to prove a classification theorem in  $\mathbb{R}^n$ . However, upon request the authors will send interested readers a computer program that calculates the list in higher dimensions by just trying a lot of random point sets; see below.

Except for the results in [Sie99] on 4 points in the plane we have no results on the number of Morse posets for  $N$  points when  $N > n + 1$ .

**5.2. Relation with computer science criteria.** In the above it was remarked that the Morse poset is a generalization of the Gabriel graph to higher dimensions. Our notion of a Morse poset, being new, has not yet an efficient stable algorithm to compute it for a general point set.

**5.3. The configuration space.** We consider the configuration space of 4 points in  $\mathbb{R}^3$ . This is  $\mathbb{R}^3$  without the generalized diagonal

$$(\mathbb{R}^3)^{(4)} = \{(P_1, P_2, P_3, P_4) \mid i \neq j \Rightarrow P_i \neq P_j\}$$

**Theorem 5.1.** *The Morse poset does not change under scaling, rotation, or translation. The quotient of  $(\mathbb{R}^3)^{(4)}$  by these group actions is a smooth 5-dimensional space.*

The proof is not very difficult, and we refrain from stating it here. The non-generic tetrahedra form a hypersurface in the configuration space. The theorem above says that there are nine different types of compartments in the complement. It does not give us any information on the number of components of the complement and their topology.

We do have the following information on the adjacency of the types of compartments, for general  $n$  and  $N = n + 1$ .

**Theorem 5.2.** *Let  $\{P(\lambda)_i\}_{i=1,\dots,n+1}$  be a generic smooth path in the configuration space, that intersects the hypersurface exactly once in the interval  $[0, 1]$ . If the Morse poset changes there is a  $j$  such that the Morse poset of  $\{P(1)_i\}_{i=1,\dots,n+1}$  has one more ( resp. one less ) active subset of length  $j$  and one more ( resp. one less ) active subset  $j + 1$  than  $\{P(0)_i\}_{i=1,\dots,n+1}$ .*

Again the proof is not very difficult, so we do not state it here.

What the theorem says for instance is that the two types  $(4, 3, 0, 0)$  with different Gabriel graphs are not adjacent.

**5.4. Statistics.** We carried out some statistical experiments to see how the different types of tetrahedra are distributed among different 4-tuples of points. In this way complement of the discriminant volume data are obtained. Four points in  $\mathbb{R}^3$  do not form a bounded space, and thus there lives no uniform probability distribution on it. As the Morse poset is invariant under translations, scaling and rotations, without loss of generality we can

assume that all 4 points lie on  $S^2$ . By translation and scaling, this can always be achieved. The ratio of the ( infinite ) volumes of the complement of the discriminant space will not change.

A reference for the following material is [Spi79], chapter 9.

In general, if one has a Riemannian manifold  $(M, g)$  the metric induces a volume form on  $M$ . The simplest Riemannian metric comes when  $M$  is embedded by a map  $\gamma$  as an orientable hypersurface in  $\mathbb{R}^n$ . Then the volume is given by:

$$\int_M \sqrt{\det(g_{ij})} dx = \int_M \|\gamma_* e_1 \wedge \cdots \wedge \gamma_* e_{n-1}\|^\frac{1}{2} dx$$

Suppose we have a map  $(\mathbb{R}/\mathbb{Z})^{n-1} \rightarrow \mathbb{R}^n$  that is onto  $M \subset \mathbb{R}^n$ . The uniform distribution on  $[0, 1]^{n-1}$  leads to a uniform distribution on  $M$  iff.  $\|\gamma_* e_1 \wedge \cdots \wedge \gamma_* e_{n-1}\|^\frac{1}{2}$  is a constant function on  $M$ . Let

$$\gamma(a_1, a_2) = (\sin(\arccos(2a_1 - 1)) \sin(2\pi a_2), \sin(\arccos(2a_1 - 1)) \cos(2\pi a_2), 2a_1 - 1)$$

With this choice it turns out that  $dV = 4\pi da_1 \wedge da_2$ . So the induced probability measure on  $S^2$  is uniform. We take two random numbers in  $[0, 1]$  and map them to  $S^2$  using  $\gamma$ .

For our experiment we used the Gnu Scientific Library, see [G<sup>+</sup>04]. This library has an implementation of the apparently very reliable MT19937 random number generator. We took samples of  $10^8$  tetrahedra. Here is one.

1	(4, 3, 0, 0) $L$	17,807,919
2	(4, 3, 0, 0) $T$	898,689
3	(4, 4, 1, 0) $O$	26,224,574
4	(4, 4, 1, 0) $P$	16,421,773
5	(4, 5, 2, 0)	24,350,101
7	(4, 4, 2, 1)	3,266,345
6	(4, 6, 3, 0)	1,797,721
8	(4, 5, 3, 1)	2,697,783
9	(4, 6, 4, 1)	6,535,095

Other samples gave approximately the same numbers, with a maximum difference of 3000.

For three random points on the circle, the chances are 50 percent that one gets an obtuse triangle. So these results are very different, and we have no explanation for them.

**5.5. Edelsbrunner ratio.** Denote, for brevity,  $d_{ij} = d(P_i, P_j)$ . The radius of the circumsphere of  $\mathbb{T}$  is  $R$ .

**Definition 5.3.** The Edelsbrunner ratio  $\rho$  is the circumradius  $R$  divided by the minimal edge length  $\min d_{ij}$ .

The ratio is used by Edelsbrunner ( see [Ede01], section 6.2 ) to classify tetrahedra into “shape types”. This article has the same objective, so it is worthwhile to compare his criterion to ours. We will show that small values of  $\rho$  can be attained by all the types listed in theorem 4.1. Depending on one’s taste one can conclude that our classification is

finer than the one proposed by Edelsbrunner, or that it describes other features. In any case, we hope to have improved on what Edelsbrunner calls a “fuzzy undertaking”.

Up to rotations and translations, the simplex is determined by the lengths of its six edges. We assume that the simplices satisfy the genericity condition 2.1. The generic simplices are an open subset  $V$  of  $(\mathbb{R}_{>0})^6$ .

**Lemma 5.4.** *Consider the circumradius  $R$  as a function of the lengths  $d_{ij}$ . It is defined when the four points are not coplanar. It is homogeneous of degree 1 and, where defined, it has nonzero gradient. In addition, on  $V$ , we have*

$$(5.1) \quad \frac{\partial R}{\partial d_{ij}} > 0 \quad 1 \leq i < j \leq 4$$

*Proof.* The first two statements are obvious. For the gradient note that

$$\sum_{1 \leq i < j \leq 4} d_{ij} \frac{\partial R}{\partial d_{ij}} = R(d_{12}, \dots, d_{34})$$

because  $R$  is homogeneous of degree one. The circumradius is always  $> 0$ , so the gradient is never zero. To see (5.1), fix the position of  $P_1, P_2$  and  $P_3$ . Varying only  $d_{34}$  the point  $P_4$  moves along a circle that has axis  $P_1P_2$ . Along this circle,  $R$  has a “maximum” when the four points are coplanar, and a “minimum” when  $P_3 = P_4$ . Both cases correspond to non-generic simplices. In between, the partial derivative of  $R$  wrt.  $d_{34}$  is clearly  $> 0$ .  $\square$

As a consequence, the Edelsbrunner ratio is a homogeneous function of degree 0. Hence, it is no restriction to assume  $R = 1$ . The above lemma says that  $\{R = 1\}$  is a smooth manifold  $W$  in  $V$ . The following lemma can also be found in [Ede01].

**Lemma 5.5.**  *$\rho$  has a unique minimum on  $W$  when all the  $d_{ij}$  are equal.*

*Proof.* Note first that it follows from (5.1) that the  $d_{ij}$  are regular functions in the sense of 2.2. We thus have six regular functions on a five dimensional space of which  $\rho$  is the maximum:

$$\rho = \max \left( \frac{1}{d_{12}}, \dots, \frac{1}{d_{34}} \right) = \frac{1}{\min(d_{12}, \dots, d_{34})}$$

Suppose that, on an open set  $V'$  in  $\mathbb{R}^N$ , we have  $N + 1$  regular functions  $f_0, \dots, f_N$ . Let  $f$  be the maximum:  $f = \max(f_0, \dots, f_N)$ . We assert that the function  $f$  can only have a minimum at  $x \in V'$  when  $f(x) = f_i(x)$ , for  $i = 0, \dots, N$ .

Indeed because the functions are regular we can assume that they are all linear functions. Our assertion is trivial in that case.

It follows that  $\rho$  can only attain its minimum when all  $d_{ij}$  are equal.  $\square$

**Lemma 5.6.** *The minimal edge length is always the length of an active edge.*

*Proof.* Suppose the minimal edge length were achieved by a non-active edge, with endpoints  $X$  and  $Y$ . The edge is not active, so inside the circumsphere corresponding to that edge there is a point that is not an endpoint of the edge. However the distance from that point to either one of the endpoints  $X$  and  $Y$  is smaller than twice the circumradius.  $\square$

**Theorem 5.7.** *On each of the compartments of the configuration space corresponding to theorem 4.1  $\rho$  is bounded from below by the values in the table below. The infimum corresponds to the quadruple of points in the third column. These quadruples lie on the discriminant hypersurface from theorem 5.2, except for the case 4641, which corresponds to the global minimum of  $\rho$ .*

Type	Rho	Infimum
(4, 3, 0, 0) $L$	$\frac{1}{2}\sqrt{3}$	$(0,0,0), (1,0,0), (1,1,0), (1,1,1)$
(4, 3, 0, 0) $T$	$\frac{1}{2}\sqrt{3}$	$(1,0,0), (0,1,0), (0,0,1), (0,0,0)$
(4, 4, 1, 0) $P$	$\sqrt{\frac{7}{12}}$	$(\frac{1}{2}\sqrt{3}, -\frac{1}{2}, 0), (-\frac{1}{2}\sqrt{3}, -\frac{1}{2}), (0,1,0), (0,1,\sqrt{3})$
(4, 4, 1, 0) $O$	$\frac{1}{2}\sqrt{2}$	$(0,0,0), (1,0,0), (1,1,0), (0,1,0)$
(4, 5, 2, 0)	$\frac{1}{2}\sqrt{2}$	$(0,0,0), (1,0,0), (1,1,0), (0,1,0)$
(4, 6, 3, 0)	$\frac{1}{2}\sqrt{2}$	$(\cos \alpha_j, \sin \alpha_j, 0) \ j = 1, \dots, 3, (0,0,1)$
(4, 4, 2, 1)	$\frac{1}{2}\sqrt{2}$	$(1,0,0), (0,1,0), (0,-1,0), (\cos \alpha, 0, \sin \alpha)$
(4, 5, 3, 1)	$\frac{1}{2}\sqrt{2}$	$(1,0,0), (0,1,0), (0,-1,0), (0,0,1)$
(4, 6, 4, 1)	$\frac{1}{4}\sqrt{6}$	$(0,1,0), (\frac{1}{2}\sqrt{3}, -\frac{1}{2}, 0), (-\frac{1}{2}\sqrt{3}, -\frac{1}{2}, 0), (0,0,\sqrt{2})$

For the case (4, 6, 3, 0) the triangle  $P_1P_2P_3$  is acute. For the case (4, 4, 2, 1) the angle  $\alpha$  should satisfy  $-\frac{\pi}{2} \leq \alpha \leq 0$ .

*Proof.* The case (4, 6, 4, 1) has been handled in the above.

Because the minimum is unique, the other cases only have an infimum for  $\rho$ . These infima should thus correspond to quadruples on the discriminant hypersurface.

The cases where  $M = 0$  are characterized by  $P_{1234} \notin \text{CH}(P_1, \dots, P_4)$ . We may assume that  $P_{1234}$  is the origin and that  $R = 1$ . It readily follows that all edges have length  $> \sqrt{2}$ . For the cases (4, 4, 1, 0)  $O$ , (4, 5, 2, 0) and (4, 6, 3, 0) the configurations in the above table show that this is actually the infimum.

If there is one triangle with an obtuse angle, we obtain in the same way that  $\rho > \frac{1}{2}\sqrt{2}$ . Thus, the configurations for (4, 4, 2, 1) and (4, 5, 3, 1) in the above table are actually infima.

We now need to study the first three cases. Let us start with (4, 4, 1, 0)  $P$ . We will assume that the triangle  $P_1P_2P_3$  is active as well as the edges  $P_1P_2$ ,  $P_1P_3$ ,  $P_1P_4$  and  $P_2P_3$ . Maximizing the minimal length of the four edges on the Gabriel graph results in four edges of equal length. Take an equilateral triangle in the plane:

$$P_1 = (0, 1, 0) \ P_2 = (-\frac{1}{2}\sqrt{3}, -\frac{1}{2}, 0) \ P_3 = (\frac{1}{2}\sqrt{3}, -\frac{1}{2}, 0)$$

This triangle has sides of length  $\sqrt{3}$ . Drawing the figure 2 in this case gives figure 4. Thus the projection of  $P_4$  to the  $P_1P_2P_3$  plane should lie in the gray area above  $P_1$  in figure 4.

Hence all cases with the projection of  $P_4$  in the colored region and  $d(P_1, P_4) = \sqrt{3}$  give (4, 4, 1, 0)  $P$ . The infimum occurs when the circumradius is minimal, and this is when  $P_4 = (0, 1, \sqrt{3})$ . In that case

$$\rho = \sqrt{\frac{7}{12}}$$

The (4, 3, 0, 0) cases. There are two cases: either none of the triangles are acute, or at

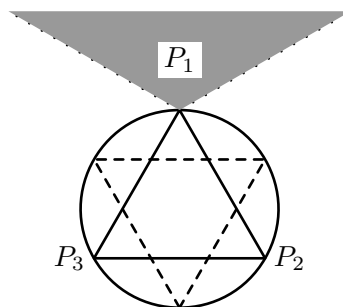


FIGURE 4. 4410P Plane

least one of the triangles is acute.

If none of the triangles are acute we look at figure 3. It follows that the projection of  $P_4$  should lie outside of the triangle  $P_1P_2P_3$ . Hence the active edges are  $P_1P_2$ ,  $P_2P_3$  and  $P_3P_4$ . To maximize the minimal edge length of these active edges, all three should have the same length, and the triangles  $P_1P_2P_3$ ,  $P_2P_3P_4$  should be right angled. The simplex is then fixed by the values in the table above.

In the second case, assume  $P_1P_2P_3$  is acute. The triangle is not active, so  $P_4$  lies inside the sphere of  $P_1P_2P_3$ . Look at figure 2. The Gabriel graph contains the smallest edges, so all the other triangles are obtuse angled. So the active edges are  $P_1P_4$ ,  $P_2P_4$  and  $P_3P_4$ . To maximize the minimal length of these edges, they should all have equal length. We see that the infimum for  $\rho$  is as in the table above.  $\square$

REMARK 5.8. With a little heuristic reasoning, omitted here, it can be argued that the configurations in the above table are actually unique infima.

## REFERENCES

- [BKOS97] M. de Berg, M. van Kreveld, M. Overmars, and O. Schwarzkopf, *Computational geometry: Algorithms and applications.*, Springer-Verlag, Heidelberg, 1997.
- [Ede01] Herbert Edelsbrunner, *Geometry and topology for mesh generation*, Cambridge Monographs on Applied and Computational Mathematics, vol. 7, Cambridge University Press, Cambridge, 2001. MR **2002k**:65206
- [G<sup>+</sup>04] M. Gallassi et al., *Gnu scientific library reference manual.*, second ed., 2004.
- [Mil63] J. Milnor, *Morse theory*, Princeton University Press, Princeton, N.J., 1963.
- [Mor59] Marston Morse, *Topologically non-degenerate functions on a compact  $n$ -manifold  $M$ .*, J. Analyse Math. **7** (1959), 189–208. MR 22 #4071
- [Mor73] ———, *F-deformations and F-tractions*, Proc. Nat. Acad. Sci. U.S.A. **70** (1973), 1634–1635. MR 47 #9631
- [Sie99] D. Siersma, *Voronoi diagrams and Morse theory of the distance function*, Geometry in Present Day Science, World Scientific, Singapore, 1999, pp. 187–208.
- [Spi79] Michael Spivak, *A comprehensive introduction to differential geometry. Vol. I*, second ed., Publish or Perish Inc., Wilmington, Del., 1979. MR **82g**:53003a

MATHEMATISCH INSTITUUT, UNIVERSITEIT UTRECHT, PO Box 80010, 3508 TA UTRECHT THE NETHERLANDS.

*E-mail address:* `siersma@math.uu.nl`

MATHEMATICAL INSTITUTE, HOKKAIDO UNIVERSITY, KITA 10, NISHI 8, KITA-KU, SAPPORO, HOKKAIDO, 060-0810, JAPAN

*E-mail address:* `manen@math.sci.hokudai.ac.jp`